Convergence on Layer-adapted Meshes and Anisotropic Interpolation Error Estimates of Non-Standard Higher Order Finite Elements

Sebastian Franz[a,1], Gunar Matthies[b,*]

[a]*Department of Mathematics and Statistics, University of Limerick, Limerick, Ireland*
[b]*Universität Kassel, Fachbereich 10 Mathematik und Naturwissenschaften, Institut für Mathematik, Heinrich-Plett-Straße 40, 34132 Kassel, Germany*

Abstract

For a general class of finite element spaces based on local polynomial spaces $\mathcal{E}$ with $\mathcal{P}_p \subset \mathcal{E} \subset \mathcal{Q}_p$ we construct a vertex-edge-cell and point-value oriented interpolation operators that fulfil anisotropic interpolation error estimates.

Using these estimates we prove ε-uniform convergence of order p for the Galerkin FEM and the LPSFEM for a singularly perturbed convection-diffusion problem with characteristic boundary layers.

Keywords: singular perturbation, characteristic layers, exponential layers, Shishkin meshes, local-projection, higher-order FEM
2000 MSC: 65N12, 65N30, 65N50

1. Introduction

We will consider the singularly perturbed convection-diffusion problem given by

$$-\varepsilon\Delta u - bu_x + cu = f \qquad \text{in } \Omega = (0,1)^2, \tag{1.1a}$$

$$u = 0 \qquad \text{on } \Gamma = \partial\Omega, \tag{1.1b}$$

under the assumption that $b \in W^1_\infty(\Omega)$ and $c \in L_\infty(\Omega)$. Additionally, let $b \geq \beta$ on $\overline{\Omega}$ with some positive constant β, while $0 < \varepsilon \ll 1$ is a small perturbation parameter.

This combination gives rise to an exponential layer of width $O(\varepsilon)$ near the outflow boundary at $x = 0$ and to two parabolic layers of width $O\left(\sqrt{\varepsilon}\right)$ near the characteristic boundaries at $y = 0$ and $y = 1$.

*Corresponding author
Email addresses: sebastian.franz@ul.ie (Sebastian Franz), matthies@mathematik.uni-kassel.de (Gunar Matthies)

[1]The author has been supported by Science Foundation Ireland under the Research Frontiers Programme 2008; Grant 08/RFP/MTH1536

Furthermore, we assume that

$$c + \tfrac{1}{2} b_x \geq c_0 > 0. \tag{1.2}$$

This ensures that problem (1.1) possesses a unique solution in $H_0^1(\Omega) \cap H^2(\Omega)$. Assumption (1.2) can always be guaranteed by a simple transformation $\tilde{u}(x, y) = u(x, y)\mathrm{e}^{\varkappa x}$ with a suitably chosen constant $\varkappa$.

The presence of layers causes that standard discretisations will not give accurate approximations on quasi uniform meshes except the mesh width is of the same order as the perturbation parameter ε. That's why layer-adapted meshes based on a priori knowledge of the solution behaviour have been constructed.

First ideas on layer-adapted meshes go back to Bakhvalov [5]. The piecewise uniform Shishkin meshes [23] were proposed originally for finite difference methods. The first analysis of finite element methods on Shishkin meshes was published in [25]. Linß combined Bakhvalov's idea to use uniform coarse meshes and graded fine meshes with Shishkin's choice of the transition point, see [16, 17].

Since the standard Galerkin methods lacks stability even on layer-adapted meshes, compare the results presented in [18], a stabilisation term will be added to the standard discretisation.

We will consider the local projection stabilisation (LPSFEM). The method is only weakly consistent, but the consistency error can be bounded such that the optimal convergence order is preserved. The local projection method provides additional control on fluctuation of certain or all derivatives and was originally proposed for the pressure stabilisation of the Stokes problem [6]. The analysis of local projection stabilisation is based on the existence of an interpolation operator which provides not only the usual estimates for the interpolation error but an additional orthogonality, see [21].

Originally, the local projection method was introduced as a two-level method. This causes the discretisation stencil to increase since additional couplings are generated by the stabilisation term. The abstract framework in [21] allows to consider also one-level local projection methods. In this case the approximation space is enriched compared to standard spaces.

In the analysis of the one-layer approach of the local projection methods, enriched Q_p-elements are used in the definition of the approximation space [19–21]. The discrete spaces are subspaces of Q_{p+1} and the purpose of the additional bubble functions is to ensure the existence of an interpolation operator with an additional orthogonality property. In [14] the authors showed that such enriched elements provide ε-uniform convergence of the Galerkin FEM and the LPSFEM of order $p + 1$. Moreover, the additional orthogonality property was not used in the proof and is therefore not needed. Hence, the enrichment can be reduced as it will be done in this paper.

We will consider in this paper higher order finite elements. To this end, we will use $p \geq 2$ to indicate the polynomial degree of our ansatz functions. The case of bilinear elements ($p = 1$) was already discussed in [14]. There it was shown that both Galerkin FEM and LPSFEM converge ε-uniformly with order one while a recovery method can achieve superconvergence of order two. Moreover, for enriched higher order elements the authors showed that the existence of suitable anisotropic interpolation error estimates yields an optimal ε-uniform convergence order for the standard Galerkin FEM and the LPSFEM on layer-adapted meshes.

The present paper can be seen as extension and continuation of [14]. We will cite several of the notations and results presented therein and consider the same class of meshes, so called S-type meshes. The main objective of this paper is to show for a wide class of finite element spaces lying between $\mathcal{P}_p$ and $\mathcal{Q}_p$ that anisotropic error estimates for at least two different kind of interpolation operators exist, one is the vertex-edge-cell interpolation while the second interpolation is based on point evaluation where the points can be chosen almost arbitrarily.

The paper is organised as follows. In Section 2 we will define a solution decomposition and the so called S-type meshes used for discretisation. The proof of ε-uniform convergence on those meshes will be given in Section 3 using a few assumptions. In Section 4 we will present a general class of finite element spaces fulfilling the assumptions of Section 3 and show the existence of at least two suitable interpolation operators, the vertex-edge-cell interpolation operator and point-value oriented interpolation operators. Moreover, we present examples of such spaces. Section 5 is devoted to numerical results confirming our theoretical results. Finally, Section 6 gives some concluding remarks.

Notation. In this paper, C denotes a generic constant which is always independent of the diffusion coefficient ε and the mesh parameter N. Although finite elements of arbitrary order are considered, the dependence of any constant on the ansatz order will not be elaborated here.

The usual Sobolev spaces $W_r^m(D)$ and $L_r(D)$ on any measurable two-dimensional subset $D \subset \Omega$ are used. We write $H^m(D)$ instead of $W_2^m(D)$ in the case $r = 2$. The $L_2(D)$-norm is denoted by $\|\cdot\|_{0,D}$ while the $(\cdot,\cdot)_D$ is the $L_2(D)$-inner product. The subscript D will always be dropped if $D = \Omega$.

By $\mathcal{P}_r(D)$ we denote the space of all polynomials with total degree less than or equal to r while $\mathcal{Q}_r(D)$ is the space of all polynomials with degree less than or equal to r in each variable separately.

Within the subsequent paper, we assume that $p \geq 2$ is an arbitrary but fixed integer.

2. Solution Decomposition and Layer-adapted Meshes

We suppose there exists a decomposition of the solution u of (1.1) into a regular solution component and various layer parts.

Assumption 1. *The solution u of* (1.1) *can be decomposed as*

$$u = v + w_1 + w_2 + w_{12}$$

where v is the regular part, w_1 is the exponential layer term of type $\mathrm{e}^{-\beta x/\varepsilon}$, w_2 the parabolic layer term of type $\mathrm{e}^{-y/\sqrt{\varepsilon}} + \mathrm{e}^{-(1-y)/\sqrt{\varepsilon}}$, and w_{12} the corner layer term of type $\mathrm{e}^{-\beta x/\varepsilon}(\mathrm{e}^{-y/\sqrt{\varepsilon}} + \mathrm{e}^{-(1-y)/\sqrt{\varepsilon}})$. We assume to have pointwise bounds on all derivatives up to order $p+1$; for a precise definition and discussion of validity see [14, Ass. 1 and Rem. 2].

When discretising (1.1), we use in both x- and y-direction so called *S-type meshes* with N mesh intervals each which are condensed in the layer regions and are equidistant outside the layer region. We will define those meshes now. For this purpose let the mesh transition parameters be

$$\lambda_x := \min\left\{\frac{1}{2}, \frac{\sigma\varepsilon}{\beta}\ln N\right\} \quad \text{and} \quad \lambda_y := \min\left\{\frac{1}{4}, \sigma\sqrt{\varepsilon}\ln N\right\}$$

with some user-chosen positive parameter $\sigma \geq p+1$. For the mere sake of simplicity in our subsequent analysis, we shall assume that

$$\lambda_x = \frac{\sigma\varepsilon}{\beta} \ln N \leq \frac{1}{2} \quad \text{and} \quad \lambda_y = \sigma\sqrt{\varepsilon} \ln N \leq \frac{1}{4}, \tag{2.1}$$

as it is typically the case for (1.1). In the following, we assume that N is a multiple of 4.

The domain Ω will be dissected by a tensor product mesh according to

$$x_i := \begin{cases} \frac{\sigma\varepsilon}{\beta}\phi\left(\frac{i}{N}\right), & i = 0, \ldots, N/2, \\ 1 - 2(1-\lambda_x)(1-\frac{i}{N}), & i = N/2, \ldots, N, \end{cases}$$

$$y_j := \begin{cases} \sigma\sqrt{\varepsilon}\phi\left(\frac{2j}{N}\right), & j = 0, \ldots, N/4, \\ (1-2\lambda_y)(\frac{2j}{N}-1)+\frac{1}{2}, & j = N/4, \ldots, 3N/4, \\ 1-\sigma\sqrt{\varepsilon}\phi\left(2-\frac{2j}{N}\right), & j = 3N/4, \ldots, N, \end{cases}$$

where ϕ is a monotonically increasing mesh-generating function satisfying $\phi(0)=0$ and $\phi(1/2)=\ln N$. Given an arbitrary function ϕ fulfilling these conditions, an S-type mesh is defined.

The final mesh is constructed by drawing lines parallel to the coordinate axes through these mesh points and is denoted by T^N. Fig. 1 shows an example of such a mesh. The domain Ω is

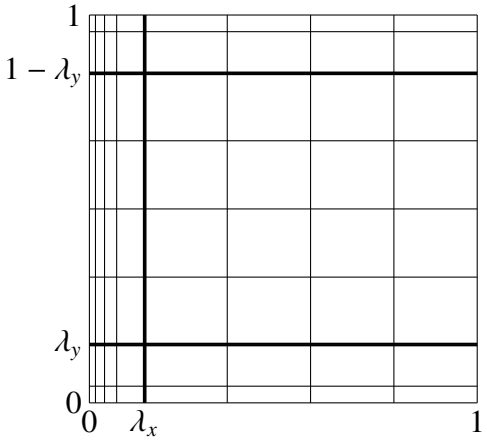

$$\Omega_{11} := [\lambda_x, 1] \times [\lambda_y, 1-\lambda_y],$$
$$\Omega_{12} := [0, \lambda_x] \times [\lambda_y, 1-\lambda_y],$$
$$\Omega_{21} := [\lambda_x, 1] \times ([0, \lambda_y] \cup [1-\lambda_y, 1]),$$
$$\Omega_{22} := [0, \lambda_x] \times ([0, \lambda_y] \cup [1-\lambda_y, 1])$$

Figure 1: Mesh T^8 of Ω, the bold lines indicate the boundaries of the subdomains.

divided into the subdomains Ω_{11}, Ω_{12}, Ω_{21}, and Ω_{22} as shown in Fig. 1, with Ω_{12} covering the exponential layer, Ω_{21} the parabolic layers, Ω_{22} the corner layers, and Ω_{11} the remaining non-layer region. Moreover, the subdomain Ω_{11} is dissected uniformly while the dissection in the other subdomains depends on ϕ.

Related to the mesh-generating function ϕ, we define by $\psi = \mathrm{e}^{-\phi}$ the mesh-characterising function ψ which is monotonically decreasing with $\psi(0) = 1$ and $\psi(1/2) = N^{-1}$. Tab. 1 gives some examples of S-type meshes using the naming convention introduced in [24]. The polynomial S-mesh has an additional parameter $m > 0$ to adjust the grading inside the layer.

The following assumptions on the mesh-generating function are needed when bounding the interpolation error.

Table 1: Some examples of mesh-generating functions ϕ and mesh-characterising functions ψ of S-type meshes, the maximum is taken on the interval $[0, 1/2]$.

Name	$\phi(t)$	$\max \phi'$	$\psi(t)$	$\max \lvert\psi'\rvert$
Shishkin mesh	$2t \ln N$	$2 \ln N$	N^{-2t}	$2 \ln N$
Bakhvalov–Shishkin mesh	$-\ln(1 - 2t(1 - N^{-1}))$	$2N$	$1 - 2t(1 - N^{-1})$	2
polynomial S-mesh	$(2t)^m \ln N$	$2m \ln N$	$N^{-(2t)^m}$	$C(\ln N)^{1/m}$
modified Bakhvalov–Shishkin mesh	$\frac{t}{q-t}$, $q = \frac{1}{2}(1 + \frac{1}{\ln N})$	$3 \ln^2 N$	$\mathrm{e}^{-\frac{t}{q-t}}$	$3/(2q) \leq 3$

Assumption 2. *Let the mesh-generating function ϕ be piecewise differentiable such that*

$$\max_{t\in[0,1/2]} \phi'(t) \leq CN \;\; \textit{or equivalently} \max_{t\in[0,1/2]} \frac{|\psi'(t)|}{\psi(t)} \leq CN$$

is fulfilled. Moreover, let the condition

$$\min_{i=1,\dots,N/2} \left(\phi\left(\frac{i}{N}\right) - \phi\left(\frac{i-1}{N}\right) \right) \geq CN^{-1}.$$

be fulfilled.

Remark 3. *The second part of Assumption 2 restricts the use of S-type meshes from Tab. 1. The original Shishkin mesh and both meshes of Bakhvalov–Shishkin type (B–S-mesh and modified B–S-mesh) fulfil Assumption 2. Unfortunately, Assumption 2 fails for the polynomial S-type meshes in the case $m > 1$.*

Notation: Let $h_i := x_i - x_{i-1}$ and $k_j := y_j - y_{j-1}$. Denote the maximal mesh sizes inside the layer regions by $h := \max_{i=1,\dots,N/2} h_i$ and $k := \max_{j=1,\dots,N/4} k_j$, by $\tau_{ij} = [x_{i-1}, x_i] \times [y_{j-1}, y_j]$ a specific cell and by τ a generic mesh rectangle. Note that the mesh cells are assumed to be closed.

3. Abstract Convergence Analysis

Without specifying the finite element space and the used interpolation operators exactly, we derive in this section bounds on the interpolation error and prove convergence of the Galerkin method and the LPSFEM based on one assumption. Let our discrete space be given by

$$V^N := \left\{ v \in H_0^1(\Omega) : v|_\tau \in \mathcal{E}(\tau) \; \forall \tau \in T^N \right\} \tag{3.1}$$

with yet unspecified local finite element spaces $\mathcal{E}(\tau)$.

With the usual Galerkin bilinear form

$$a_{Gal}(u, v) := \varepsilon(\nabla u, \nabla v) + (cu - bu_x, v), \qquad u, v \in H_0^1(\Omega),$$

associated with problem (1.1), a weak formulation of the convection-diffusion problem (1.1) reads:

Find $u \in H_0^1(\Omega)$ such that

$$a_{Gal}(u, v) = (f, v) \qquad \forall v \in H_0^1(\Omega) \tag{3.2}$$

and the standard Galerkin formulation of (1.1) is given by

Find $\tilde{u}^N \in V^N$ such that

$$a_{Gal}(\tilde{u}^N, v^N) = (f, v^N) \qquad \forall v^N \in V^N. \tag{3.3}$$

Due to (1.2), problems (3.2) and (3.3) possess a unique solution each.

Since the standard Galerkin discretisation lacks stability even on S-type meshes, see the numerical results given in [18], the local projection method is applied for stabilisation. To this end, we introduce some more notation. Let π_τ denote the L_2-projection into the finite dimensional function space $D(\tau) = \mathcal{P}_{p-2}(\tau)$. The fluctuation operator $\kappa_\tau : L_2(\tau) \to L_2(\tau)$ is defined by $\kappa_\tau v := v - \pi_\tau v$. In order to get additional control on the derivative in streamline direction, we define the stabilisation term

$$s(u, v) := \sum_{\tau \in T^N} \delta_\tau (\kappa_\tau(bu_x), \kappa_\tau(bv_x))_\tau$$

with the nonnegative cell-dependent parameters δ_τ, $\tau \in T^N$, which will be specified later in the analysis, see Theorem 6. The parameter will be constant inside each subdomain of Ω, i.e. $\delta_\tau = \delta_{ij}$ for $\tau \subset \Omega_{ij}$. It was stated in [11, 12] for different stabilisation methods that stabilisation is best if only applied in $\Omega_{11} \cup \Omega_{21}$. Therefore, we set $\delta_{12} = \delta_{22} = 0$ in the following.

An alternative way for stabilisation would be to add the term

$$g(u, v) = \sum_{\tau \in T^N} \delta_\tau (\kappa_\tau(\nabla u), \kappa_\tau(\nabla v))_\tau.$$

Using the stabilisation term g within a local projection method for problems with characteristic layers would lead to a different scaling of the stabilisation parameter δ_{21} which would be proportional to $\varepsilon^{1/2}$ (using g) instead of $\varepsilon^{-1/2}$ (using s). The scaling $\delta_{21} \sim \varepsilon^{-1/2}$ for the stabilisation term s will be shown in Theorem 6, see (3.9b).

The stabilised bilinear form a_{LPS} is defined by

$$a_{LPS}(u, v) := a_{Gal}(u, v) + s(u, v), \qquad u, v \in H_0^1(\Omega),$$

and the stabilised discrete problem reads:

Find $u^N \in V^N$ such that

$$a_{LPS}(u^N, v^N) = (f, v^N) \qquad \forall v^N \in V^N. \tag{3.4}$$

The subsequent analysis uses the ε-weighted energy norm

$$|||v|||_\varepsilon := \left(\varepsilon \|\nabla v\|_0^2 + c_0 \|v\|_0^2\right)^{1/2}$$

and the LPS-norm

$$|||v|||_{LPS} := \left(\varepsilon\|\nabla v\|_0^2 + c_0\|v\|_0^2 + s(v,v)\right)^{1/2}.$$

We now come to the properties of the underlying discrete space V^N. The following assumption on our discrete space is the foundation of the interpolation error bounds and the convergence proof later on.

Assumption 4. *There exists an interpolation operator $I^N : C(\overline{\Omega}) \to V^N$ such that the stability property*

$$\left\|I^N w\right\|_{L_\infty(\tau)} \leq C\|w\|_{L_\infty(\tau)} \quad \forall w \in C(\tau),\ \forall \tau \subset \overline{\Omega}, \tag{3.5}$$

and the anisotropic error estimates

$$\left\|w - I^N w\right\|_{L_q(\tau_{ij})} \leq C \sum_{r=0}^{s} \left\| h_i^{s-r} k_j^r \frac{\partial^s w}{\partial x^{s-r}\partial y^r} \right\|_{L_q(\tau_{ij})}, \tag{3.6a}$$

$$\left\|(w - I^N w)_x\right\|_{L_q(\tau_{ij})} \leq C \sum_{r=0}^{t} \left\| h_i^{t-r} k_j^r \frac{\partial^{t+1} w}{\partial x^{t-r+1}\partial y^r} \right\|_{L_q(\tau_{ij})} \tag{3.6b}$$

and similarly for the y-derivative hold true for $\tau_{ij} \subset \overline{\Omega}$ and $q \in [1,\infty]$, $2 \leq s \leq p+1$, $1 \leq t \leq p$.

Remark 5. *This assumption depends only on the definition of our local finite element space $\mathcal{E}(\tau)$. For the standard Q_p-space, Assumption 4 holds for the vertex-edge-cell interpolation operator, see [26]. Similar results using the standard Lagrange interpolation can be found in [2].*

With these local assumptions we derive directly from [14, Theorem 12] interpolation error bounds of order $p+1$ in the L_∞-norm and of order p in the energy norm, and convergence of order p for the Galerkin FEM and the stabilised LPSFEM in the energy norm. Moreover, the LPSFEM shows a convergence order p in the local projection norm for the closeness error. We cite [14, Theorems 13 and 15] here.

Theorem 6 (Convergence Galerkin FEM and LPSFEM). *Let the solution u of* (3.2) *satisfy Assumption 1 and let $\tilde{u}^N$ denote the Galerkin solution of* (3.3)*. We set*

$$C_\psi := 1 + N^{-1/2}\ln^{1/2} N \max|\psi'|. \tag{3.7}$$

Then, we have

$$\left|\left|\left|u - \tilde{u}^N\right|\right|\right|_\varepsilon \leq CC_\psi(h + k + N^{-1}\max|\psi'|)^p. \tag{3.8}$$

Let the LPSFEM solutions of (3.4) *be denoted by u^N and let the stabilisation parameters be chosen according to*

$$\delta_{11} \leq CN^{-2}(\max|\psi'|)^{2p}, \tag{3.9a}$$

$$\delta_{21} \leq C\varepsilon^{-1/2}\ln^{-1} N(k + N^{-1}\max|\psi'|)^2, \tag{3.9b}$$

$$\delta_{12} = \delta_{22} = 0. \tag{3.9c}$$

Then, we have

$$\left|\!\left|\!\left|u - u^N\right|\!\right|\!\right|_\varepsilon \leq CC_\psi(h + k + N^{-1}\max|\psi'|)^p \tag{3.10}$$

and

$$\left|\!\left|\!\left|I^N u - u^N\right|\!\right|\!\right|_{LPS} \leq CC_\psi(h + k + N^{-1}\max|\psi'|)^p. \tag{3.11}$$

Remark 7. *The factor C_ψ defined in* (3.7) *is bounded by a constant for all meshes considered in Table 1. Nevertheless, there are S-type meshes which fulfil Assumption 2 but provide $C_\psi \to \infty$ as $N \to \infty$. For example, let $\xi_0 := \frac{1}{2}(1 - N^{-1}\ln N)$ and define for $k > 2$*

$$\phi(t) = \begin{cases} \dfrac{t\ln N}{k\xi_0}, & 0 \leq t \leq \xi_0, \\ N(2t-1)(1-1/k) + \ln N, & \xi_0 \leq t \leq \frac{1}{2}. \end{cases}$$

Here $\max|\psi'| \geq |\psi'(\xi_0+)| = 2(1-1/k)N^{1-1/k}$. Hence, C_ψ will increase with increasing N for this type of meshes.

4. Anisotropic Interpolation on Finite Element Spaces

In this section we will define a general finite element that allows us to generate finite element spaces such that at least two different interpolation operators fulling Assumption 4 exist. Moreover, examples for the general finite element will be given.

We will make use of the approach in [2] to prove the anisotropic error estimates (3.6). For this purpose, let $\hat{\tau} = [-1,1]^2$ denote the reference element, $\widehat{\mathcal{E}}(\hat{\tau})$ be the local polynomial element space on the reference element, γ a multiindex, and D^γ the corresponding differential operator. Moreover, we set $m = |\gamma|$, $d = \dim(D^\gamma\widehat{\mathcal{E}}(\hat{\tau}))$, and (ξ,η) denote the coordinates on the reference element $\hat{\tau}$.

The task of proving Assumption 4 to be fulfilled reduces to finding sets $\mathcal{F} = \{F_i\}$ of d linearly independent functionals such that

$$F_i \in (W_q^{p+1-m}(\hat{\tau}))' \qquad \forall i = 1,\dots,d, \tag{4.1a}$$

$$F_i(D^\gamma(\hat{v} - \hat{I}\hat{v})) = 0 \qquad \forall i = 1,\dots,d, \forall \hat{v} \in C(\hat{\tau}) :\ D^\gamma\hat{v} \in W_q^{p+1-m}(\hat{\tau}), \tag{4.1b}$$

$$\hat{w} \in \widehat{\mathcal{E}}(\hat{\tau}) \text{ and } F_i(D^\gamma\hat{w}) = 0 \quad \forall i = 1,\dots,d \Rightarrow\ D^\gamma\hat{w} = 0. \tag{4.1c}$$

Assumption 4 then follows by [2, Lemma 2.15] for $\mathcal{P}_p(\hat{\tau}) \subset \widehat{\mathcal{E}}(\hat{\tau})$. Note that in [1, 26] for $\widehat{\mathcal{E}}(\hat{\tau}) = \mathcal{Q}_p(\hat{\tau})$ and a vertex-edge-cell interpolation operator such sets of functionals are given. In [14, 19] an enriched $\mathcal{Q}_p(\hat{\tau})$-element was studied and functionals were given.

Here we want to study finite element spaces that are subspaces of $\mathcal{Q}_p(\hat{\tau})$. Therefore the resulting elements can be seen as reduced $\mathcal{Q}_p$-elements. Due to $\mathcal{P}_p(\hat{\tau}) \subset \widehat{\mathcal{E}}(\hat{\tau})$, they are also enriched $\mathcal{P}_p$-elements.

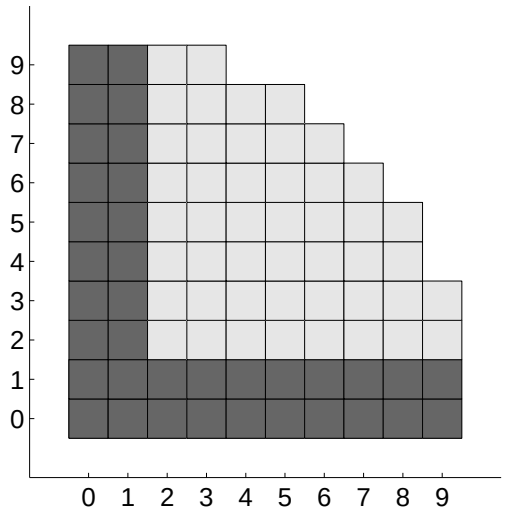

Figure 2: General element space $Q_p^{\clubsuit}(\hat{\tau})$ with some arbitrary space $\widetilde{Q}(\hat{\tau})$ for $p = 9$.

Note that all the following local function spaces can be combined in a continuous way to form a continuous finite element space V^N, see (3.1), since the restriction of the function spaces to an edge E is always $\mathcal{P}_p(E)$.

Define the general element space by

$$Q_p^{\clubsuit}(\hat{\tau}) = \operatorname{span}\Big\{\{1,\xi\}\times\{1,\eta,\dots,\eta^p\}\cup\{1,\xi,\dots,\xi^p\}\times\{1,\eta\}\cup\xi^2\eta^2\widetilde{Q}(\hat{\tau})\Big\}$$

where the space $\widetilde{Q}(\hat{\tau}) \subset Q_{p-2}(\hat{\tau})$ is given by

$$\widetilde{Q}(\hat{\tau}) = \operatorname{span}\Big\{\xi^i\eta^j \;:\; i = 0,\dots,p-2,\; j = 0,\dots,k_i\Big\}$$

with $k_i \geq k_{i+1}$, $i = 0,\dots,p-3$. Hence, $\xi^i\eta^j \in \widetilde{Q}(\hat{\tau})$ implies $\xi^a\eta^j, \xi^i\eta^b \in \widetilde{Q}(\hat{\tau})$ for $0 \leq a < i$ and $0 \leq b < j$. Furthermore, the space $Q_p^{\clubsuit}(\hat{\tau})$ can be written as

$$Q_p^{\clubsuit}(\hat{\tau}) = \operatorname{span}\Big\{\{1,\xi\}\times\{1,\eta,\dots,\eta^p\}\cup\{1,\xi,\dots,\xi^p\}\times\{1,\eta\}\cup(1-\xi^2)(1-\eta^2)\widetilde{Q}(\hat{\tau})\Big\} \tag{4.2}$$

and its dimension is given by

$$\big|\widetilde{Q}(\hat{\tau})\big| = \sum_{i=0}^{p-2}(k_i+1)_+, \quad \text{where } (\cdot)_+ = \max\{\cdot,0\}.$$

Figure 2 shows a graphical representation of an example of $Q_p^{\clubsuit}(\hat{\tau})$ in the case $p = 9$. A square at position (i, j) represents a basis function $\xi^i\eta^j$ of $Q_p^{\clubsuit}(\hat{\tau})$. The darker squares correspond to those functions present in all spaces we consider, while the lighter ones represent $\xi^2\eta^2\widetilde{Q}(\hat{\tau})$. In order to incorporate [2], we need $\mathcal{P}_p(\hat{\tau}) \subset Q_p^{\clubsuit}(\hat{\tau})$ which is automatically satisfied for $p \leq 3$. For $p \geq 4$, the inclusion $\mathcal{P}_{p-4}(\hat{\tau}) \subset \widetilde{Q}(\hat{\tau})$ has to be fulfilled.

4.1. Vertex-edge-cell interpolation operator

In this subsection, we consider a vertex-edge-cell interpolation operator which is based on point evaluation at the vertices, line integrals along the edges and integrals over the cell interior.

Let $\hat{a}_i$ and $\hat{e}_i$, $i = 1, \dots, 4$, denote the vertices and edges of $\hat{\tau}$, respectively. We define the vertex-edge-cell interpolation operator $\hat{I} : C(\hat{\tau}) \to Q_p^{\clubsuit}(\hat{\tau})$ by

$$\hat{I}\hat{v}(\hat{a}_i) = \hat{v}(\hat{a}_i), \quad i = 1, \dots, 4, \tag{4.3a}$$

$$\int_{\hat{e}_i} (\hat{I}\hat{v})\hat{q} = \int_{\hat{e}_i} \hat{v}\hat{q}, \quad i = 1, \dots, 4, \quad \hat{q} \in \mathcal{P}_{p-2}(\hat{e}_i), \tag{4.3b}$$

$$\iint_{\hat{\tau}} (\hat{I}\hat{v})\hat{q} = \iint_{\hat{\tau}} \hat{v}\hat{q}, \qquad \hat{q} \in \widetilde{Q}(\hat{\tau}). \tag{4.3c}$$

Similar to [20, Lemma 3], it can be proved that this interpolation operator is uniquely defined and can be extended to the global interpolation operator $I^N : C(\overline{\Omega}) \to V^N$ by

$$(I^N v)|_\tau := (\hat{I}(v \circ F_\tau)) \circ F_\tau^{-1} \quad \forall \tau \in T^N,\ v \in C(\overline{\Omega}), \tag{4.4}$$

with the bijective reference mapping $F_\tau : \hat{\tau} \to \tau$. Stability (3.5) can be proved similarly to [20]. For the anisotropic error estimates (3.6) we define two sets of functionals, one in the case $\gamma = (0, 0)$ and one for $\gamma = (1, 0)$. The third case $\gamma = (0, 1)$ follows analogously.

Functionals for $\gamma = (0, 0)$

Based on the definition (4.3) of the interpolation operator $\hat{I}$, let the functionals be given by

$$\hat{v} \mapsto \hat{v}(a_i), \quad i = 1, \dots, 4, \tag{4.5a}$$

$$\hat{v} \mapsto \int_{\hat{e}_i} \hat{v}q, \quad i = 1, \dots, 4, \quad q \in \mathcal{P}_{p-2}(\hat{e}_i), \tag{4.5b}$$

$$\hat{v} \mapsto \iint_{\hat{\tau}} \hat{v}q, \quad q \in \widetilde{Q}(\hat{\tau}). \tag{4.5c}$$

We have $4 + 4(p-1) + |\widetilde{Q}(\hat{\tau})| = |Q_p^{\clubsuit}(\hat{\tau})|$ functionals. They are defined by point evaluation and integrals, and therefore (4.1a) holds. Condition (4.1b) follows immediately since the used functionals are covered by the point and integral evaluation given in the definition (4.3) of $\hat{I}$. For (4.1c) assume $w \in Q_p^{\clubsuit}(\hat{\tau})$ with all above functionals applied to it being zero. By (4.5a) and (4.5b) we obtain $w|_{\partial\hat{\tau}} \equiv 0$. Thus, $w = (1-\xi^2)(1-\eta^2)q$ with $q \in \widetilde{Q}(\hat{\tau})$ due to (4.2). Then by (4.5c) follows $w \equiv 0$.

Functionals for $\gamma = (1, 0)$

Let $W = \partial_\xi(Q_p^{\clubsuit}(\hat{\tau}))$. Its dimension is given by $|Q_p^{\clubsuit}(\hat{\tau})| - (p+1) = 3p - 1 + |\widetilde{Q}(\hat{\tau})|$. For the definition of the functionals we follow [1]. Let S be the set of the two edges of $\hat{\tau}$ parallel to the ξ-axis. Consider the functionals

$$\hat{v} \mapsto \int_{\hat{e}} vq, \quad q \in \mathcal{P}_{p-1}(\hat{e}),\ \hat{e} \in S, \tag{4.6a}$$

$$\hat{v} \mapsto \iint_{\hat{\tau}} vq, \quad q \in \partial_\xi \partial_\eta^2 Q_p^{\clubsuit}(\hat{\tau}). \tag{4.6b}$$

We have $2p + |\widetilde{Q}(\hat{\tau})| + p - 1 = |W|$ functionals and similar arguments as before show (4.1a). Adapting the method of [1, Section 2.4], using $\partial_\xi \partial_\eta^2 Q_p^\clubsuit(\hat{\tau}) = \operatorname{span}\left\{1, \eta, \ldots, \eta^{p-2}\right\} \cup \xi\widetilde{Q}(\hat{\tau})$ and integration by parts shows (4.1b). For the linear independence consider $\hat{v} \in \partial_\xi Q_p^\clubsuit(\hat{\tau})$ with all above functionals applied to it being zero. Then (4.6a) yields $\hat{v} \equiv 0$ for $|\eta| = 1$. Thus $\hat{v} = (1 - \eta^2)q$ with $q \in \partial_\xi \partial_\eta^2 Q_p^\clubsuit(\hat{\tau})$. Now (4.6b) gives $v \equiv 0$ in $\hat{\tau}$, which is (4.1c). Thus

Theorem 8. *For the finite element space*

$$V^N = \{v \in C(\Omega) : v|_\tau \in Q_p^\clubsuit(\tau) \ \forall \tau \in T^N\}$$

and the vertex-edge-cell interpolation operator I^N defined by (4.3) *and* (4.4)*, the Assumption 4 holds true.*

4.2. Point-value oriented interpolation

In this subsection, we will show that also point-value oriented interpolation operators can provide the anisotropic interpolation error estimates of Assumption 4.

Let $-1 = \xi_0 < \xi_1 < \cdots < \xi_{p-1} < \xi_p = +1$ and $-1 = \eta_0 < \eta_1 < \cdots < \eta_{p-1} < \eta_p = +1$ be two increasing sequences of $p+1$ points of $[-1, +1]$ which include both end points. We define the point-value oriented interpolation operator $\hat{J} : C(\hat{\tau}) \to Q_p^\clubsuit(\hat{\tau})$ by values at the vertices

$$(\hat{J}\hat{v})(\pm 1, -1) := \hat{v}(\pm 1, -1), \qquad (\hat{J}\hat{v})(\pm 1, +1) := \hat{v}(\pm 1, +1) \tag{4.7a}$$

values on the edges

$$\left.\begin{aligned} (\hat{J}\hat{v})(\xi_i, \pm 1) &:= \hat{v}(\xi_i, \pm 1), \qquad i = 1, \ldots, p-1, \\ (\hat{J}\hat{v})(\pm 1, \eta_j) &:= \hat{v}(\pm 1, \eta_j), \qquad j = 1, \ldots, p-1, \end{aligned}\right\} \tag{4.7b}$$

and values in the interior

$$(\hat{J}\hat{v})(\xi_{i+1}, \eta_{j+1}) := \hat{v}(\xi_{i+1}, \eta_{j+1}), \qquad i = 0, \ldots, p-2, \, j = 0, \ldots, k_i. \tag{4.7c}$$

It remains to show that these interpolation conditions provide a uniquely determined interpolation operator. To this end, let $\hat{v} \in Q_p^\clubsuit(\hat{\tau})$ be a polynomial which vanishes at all above points. The restriction $\hat{v}|_{\hat{e}_i}$ of $\hat{v}$ onto an edge $\hat{e}_i$ of the reference square belongs to $P_p(\hat{e}_i)$ since $Q_p^\clubsuit(\hat{\tau}) \subset Q_p(\hat{\tau})$. However, the restriction vanishes in $(p+1)$ points. Hence, the polynomial $\hat{v}$ vanishes on each edge $\hat{e}_i$ of the boundary $\partial\hat{\tau}$ and with (4.2) holds

$$\hat{v} = (1 - \xi^2)(1 - \eta^2)\hat{w}, \qquad \hat{w} \in \widetilde{Q}(\hat{\tau}),$$

where the polynomial $\hat{w}$ vanishes at all interior interpolation points. If $k_0 < 0$ we obtain $\widetilde{Q}(\hat{\tau}) = \{0\}$ and therefore $\hat{w} \equiv 0$ which implies $\hat{v} \equiv 0$. Otherwise, from $k_i \geq k_{i+1}$, $i = 0, \ldots, p-3$, we conclude that the restriction of $\hat{w}$ onto the line $\xi = \xi_1$ is a polynomial of degree $k_0 \geq 0$ in η. This polynomial vanishes at $(k_0 + 1)$ points and therefore

$$\hat{w} = (\xi - \xi_1)\hat{w}_1, \qquad \hat{w}_1 \in \widetilde{Q}_1 = \operatorname{span}\left\{\bigcup_{i=1}^{p-2}\bigcup_{j=0}^{k_i} \xi^i - 1\eta^j\right\}.$$

If $k_1 < 0$ we obtain $\widetilde{Q}_1 = \{0\}$ and therefore $\hat{w}_1 \equiv 0$ which implies $\hat{v} \equiv 0$. Otherwise, $\hat{w}_1$ vanishes at all interior interpolation points (ξ_i, η_j) with $i > 2$. The restriction of $\hat{w}_1$ onto the line $\xi = \xi_2$ is a polynomial of degree at most $k_1 \geq 0$ in η vanishing at $(k_1 + 1)$ points. Hence,

$$\hat{w}_1 = (\xi - \xi_2)\hat{w}_2, \qquad \hat{w}_2 \in \widetilde{Q}_2 = \operatorname{span}\left\{ \bigcup_{i=2}^{p-2} \bigcup_{j=0}^{k_i} \xi^i - 2\eta^j \right\}.$$

The procedure is continued. Let $m = \max\{i : k_i \geq 0\} \leq p - 2$. We get for $\ell = 2, \ldots, m$

$$\hat{w}_\ell = (\xi - \xi_{\ell+1})\hat{w}_{\ell+1}, \qquad \hat{w}_{\ell+1} \in \widetilde{Q}_{\ell+1} = \operatorname{span}\left\{ \bigcup_{i=\ell+1}^{p-2} \bigcup_{j=0}^{k_i} \xi^i - (\ell+1)\eta^j \right\}$$

and

$$\hat{w}_{m+1} \in \widetilde{Q}_{m+1} = \operatorname{span}\left\{ \bigcup_{i=m+1}^{p-2} \bigcup_{j=0}^{k_i} \xi^i - (m+1)\eta^j \right\} = \{0\}.$$

Therefore $\hat{w}_{m+1} \equiv 0$ which implies $v \equiv 0$. This means that the interpolation operator $\widehat{J}$ is uniquely determined.

The global interpolation operator $J^N : C(\overline{\Omega}) \to V^N$ is given by

$$(J^N v)|_\tau := (\hat{J}(v \circ F_\tau)) \circ F_\tau^{-1}, \qquad \tau \in T^N, v \in C(\overline{\Omega}), \tag{4.8}$$

where F_τ is again the bijective reference mapping.

The anisotropic estimate for the interpolation error in the case $\gamma = (0, 0)$ follows immediately from the definition of $\hat{J}$ which is based on point evaluation.

We will prove the anisotropic error estimates for the case $\gamma = (0, 1)$ only since the case $\gamma = (1, 0)$ follows in a similar way. Let $W = \partial_\eta(\mathcal{Q}_p^\clubsuit(\hat{\tau}))$ with $|W| = |\mathcal{Q}_p^\clubsuit(\hat{\tau})| - (p+1) = 3p - 1 + |\widetilde{Q}(\hat{\tau})|$. We define the set $\mathcal{G}$ by the functionals

$$\hat{v} \mapsto \int_{-1}^{\eta_j} \hat{v}(\pm 1, \eta)\, d\eta, \qquad j = 1, \ldots, p, \tag{4.9a}$$

$$\hat{v} \mapsto \int_{-1}^{\eta_{j+1}} \hat{v}(\xi_{i+1}, \eta)\, d\eta, \qquad i = 0, \ldots, p-2, j = p \text{ and if } k_i \geq 0 : \ j = 0, \ldots, k_i. \tag{4.9b}$$

Note that

$$|\mathcal{G}| = 2p + \sum_{i=0}^{p-2}((k_i + 1)_+ + 1) = 3p - 1 + |\widetilde{Q}(\hat{\tau})| = |W|.$$

All functionals in $\mathcal{G}$ are integrals along vertical lines and therefore condition (4.1a) is satisfied. In order to prove (4.1b), let $G \in \mathcal{G}$ be an arbitrary functional. This means that

$$G\hat{v} = \int_{-1}^{b} \hat{v}(a, \eta)\, d\eta$$

where $a = \xi_i$ for some $i \in \{0, \dots, p\}$ and $b = \eta_j$ for some $j \in \{1, \dots, p\}$. Concerning (4.1b), we obtain

$$G((\hat{J}\hat{v} - \hat{v})_\eta) = \int_{-1}^{b} (\hat{J}\hat{v} - \hat{v})_\eta(a, \eta)\, d\eta = (\hat{J}\hat{v} - \hat{v})(a, \eta)\Big|_{\eta=-1}^{b} = 0$$

since both points $(a, -1)$ and (a, b) belong to the set of points which are used to define the interpolation operator. Hence, condition (4.1b). Since all nodal functionals in $\mathcal{G}$ are integrals along different vertical lines they are linearly independent on $C^\infty(\hat{\tau})$. Hence, also condition (4.1c) is fulfilled.

Theorem 9. *The finite element space V^N together with the point-value oriented interpolation operator J^N defined by* (4.7) *and* (4.8) *provides the anisotropic interpolation error estimates of Assumption 4.*

Remark 10. *In cases where $\widetilde{Q}(\hat{\tau})$ cannot be represented by monomials in the assumed way, the above proofs become more difficult. The main task will be the proof of the unisolvence of the interpolation operators $\hat{I}$ and $\hat{J}$.*

4.3. Examples of Polynomial Spaces

In the this subsection we will give several examples of polynomial spaces fitting in the framework presented. In particular, the structural assumption on $\widetilde{Q}(\hat{\tau})$ is fulfilled.

Full Space Q_p

If we take

$$\widetilde{Q}(\hat{\tau}) = Q_{p-2}(\hat{\tau})$$

then we have as local polynomial space

$$Q_p(\hat{\tau}) = \operatorname{span}\Big\{\{1, \xi, \dots, \xi^p\} \times \{1, \eta, \dots, \eta^p\}\Big\},$$

see Figure 3.

The proof that Assumption 4 is fulfilled can also be found in [26] for I^N according to (4.3), (4.4) and in [2] for J^N according to (4.7), (4.8).

Enriched Space Q_p^+

In [14] the standard Q_{p-1}-space was enriched by 6 functions to form a space Q_p^+. In terms of the general definition it can be described using

$$\widetilde{Q}(\hat{\tau}) = Q_{p-3}(\hat{\tau}) \oplus \operatorname{span}\Big\{\xi^{p-2}, \eta^{p-2}\Big\} \tag{4.10}$$

and therefore

$$\begin{aligned} Q_p^+(\hat{\tau}) = Q_{p-1}(\hat{\tau}) &\oplus \operatorname{span}\Big\{(1-\xi^2)(1-\eta^2)\xi^{p-2}, (1-\xi^2)(1-\eta^2)\eta^{p-2}\Big\} \\ &\oplus \operatorname{span}\Big\{(1+\xi)(1-\eta^2)\eta^{p-2}, (1-\xi)(1-\eta^2)\eta^{p-2}, \\ &\qquad (1+\eta)(1-\xi^2)\xi^{p-2}, (1-\eta)(1-\xi^2)\xi^{p-2}\Big\}, \end{aligned}$$

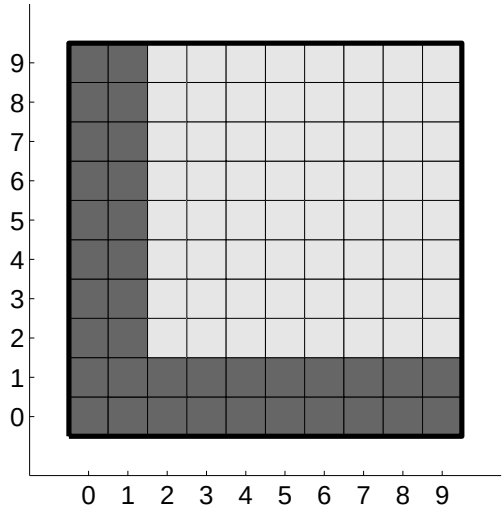

Figure 3: Full space $Q_p(\hat{\tau})$ by choosing $\widetilde{Q}(\hat{\tau}) = Q_{p-2}(\hat{\tau})$ for $p = 9$.

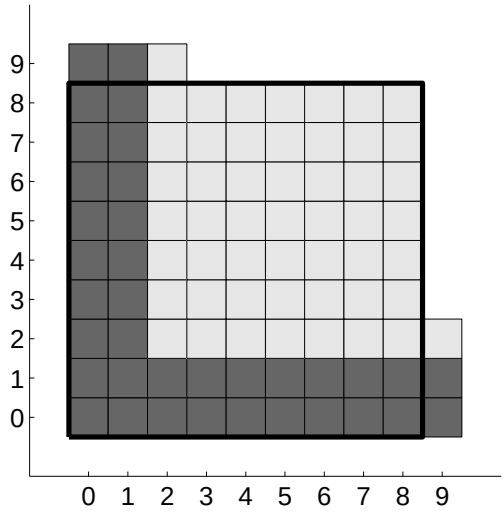

Figure 4: Enriched space $Q_p^+(\hat{\tau})$ by choosing $\widetilde{Q}(\hat{\tau})$ according to (4.10) for $p = 9$.

see also Figure 4.

This space yields

$$\mathcal{P}_p \subset Q_p^+ \subset Q_p$$

and Assumption 4 holds true, see also [14] for I^N according to (4.3), (4.4).

Reduced Enrichment Space Q_p^*

We will now give a smaller enrichment of the space $Q_{p-1}(\hat{\tau})$—an enrichment with only 4 additional functions. In order to have $Q_{p-1}(\hat{\tau}) \subset \mathcal{E}(\hat{\tau})$ we take

$$\widetilde{Q}(\hat{\tau}) = Q_{p-3}(\hat{\tau}).$$

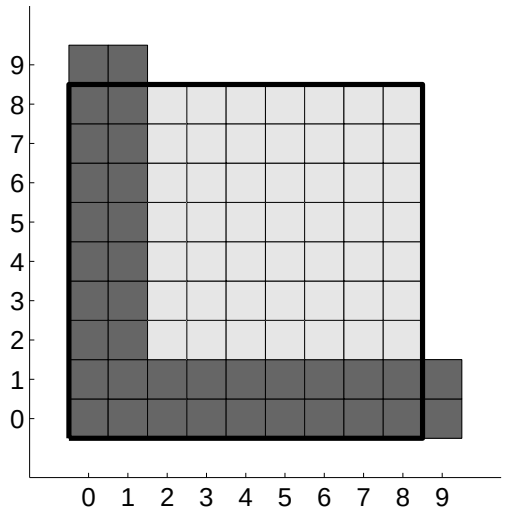

Figure 5: Enriched space $\mathcal{Q}_p^*(\hat{\tau})$ by choosing $\widetilde{\mathcal{Q}}(\hat{\tau}) = \mathcal{Q}_{p-3}(\hat{\tau})$ for $p = 9$.

Then the enriched space $\mathcal{Q}_p^*(\hat{\tau})$ is given by

$$\mathcal{Q}_p^*(\hat{\tau}) = \mathcal{Q}_{p-1}(\hat{\tau}) \oplus \operatorname{span}\Big\{(1+\xi)(1-\eta^2)\eta^{p-2}, (1-\xi)(1-\eta^2)\eta^{p-2}, \\ (1+\eta)(1-\xi^2)\xi^{p-2}, (1-\eta)(1-\xi^2)\xi^{p-2}\Big\},$$

see Figure 5. This enriched finite element space yields

$$\mathcal{P}_p \subset \mathcal{Q}_p^* \subset \mathcal{Q}_p^+ \subset \mathcal{Q}_p$$

and

$$\mathcal{Q}_{p-1} \subset \mathcal{Q}_p^*.$$

The space $\mathcal{Q}_p^*$ is the smallest space having $\mathcal{Q}_{p-1}$ as subspace and fulfilling Assumption 4.

Serendipity Space $\mathcal{Q}_p^\oplus$

The minimal element space is governed by taking

$$\widetilde{\mathcal{Q}}(\hat{\tau}) = \mathcal{P}_{p-4}(\hat{\tau}) \text{ for } p \geq 4$$

and $\widetilde{\mathcal{Q}}(\hat{\tau}) = \emptyset$ for $p = 2, 3$. It can be seen as enriching $\mathcal{P}_p$ with two edge-bubble functions,

$$\mathcal{Q}_p^\oplus(\hat{\tau}) = \mathcal{P}_p(\hat{\tau}) \oplus \operatorname{span}\Big\{(1+\xi)(1-\eta^2)\eta^{p-2}, (1+\eta)(1-\xi^2)\xi^{p-2}\Big\},$$

see also Figure 6.

This minimal element is known under different names, e.g. "trunk element" or "serendipity element" [3, 4, 22, 27]. It is the continuous quadrilateral element with the fewest degrees of freedom containing $\mathcal{P}_p$.

It holds

$$\mathcal{P}_p \subset \mathcal{Q}_p^\oplus \subset \mathcal{Q}_p^* \subset \mathcal{Q}_p^+ \subset \mathcal{Q}_p.$$

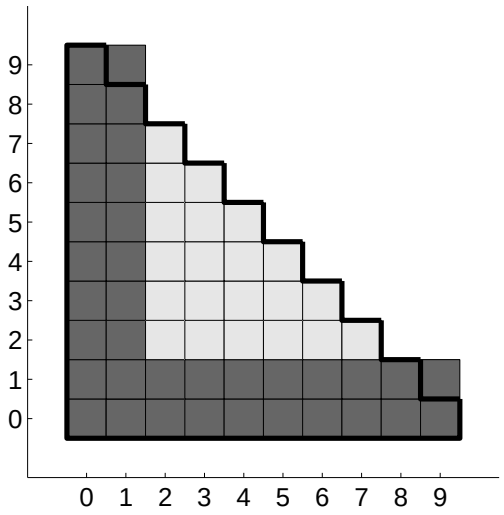

Figure 6: Serendipity space $Q_p^{\oplus}(\hat{\tau})$ by choosing $\widetilde{Q}(\hat{\tau}) = \mathcal{P}_{p-4}(\hat{\tau})$ for $p = 9$.

Remark 11. *Consider an $N \times N$ S-type mesh. In Table 2 we compare the number of degrees of freedom for the different spaces given. In the second column the number of degrees of freedom (d.o.f.) for an arbitrary order $p \geq 3$ on each element is given. For $p = 2$ the formulas are different because $Q_2^+ = Q_2$ and $Q_2^* = Q_2^{\oplus}$. The overall number of d.o.f. on the mesh is given in the third column. Due to continuity it is less than $(N + 1)^2$ times the second column. We present only the leading term in N; the remaining terms are $2pN + 1$ for all spaces. Finally, the last two columns show for the choices $p = 3$ and $p = 5$ the reduction in degrees of freedom. The serendipity space $Q_p^{\oplus}$ needs about half the number compared to the space Q_p.*

Table 2: Comparing the number of degrees of freedom for the different finite element spaces

space	d.o.f. per element	d.o.f. on $N \times N$-mesh	$p = 3$	$p = 5$
Q_p	$(p+1)^2$	p^2N^2	$9N^2$	$25N^2$
Q_p^+	$p^2 + 6$	$(p^2 - 2p + 5)N^2$	$8N^2$	$20N^2$
Q_p^*	$p^2 + 4$	$(p^2 - 2p + 3)N^2$	$6N^2$	$18N^2$
$Q_p^{\oplus}$	$\frac{(p+1)(p+2)}{2} + 2$	$\frac{p(p-1)+4}{2}N^2$	$5N^2$	$12N^2$

5. Numerical Results

We consider as numerical example the singularly perturbed convection-diffusion problem

$$\begin{aligned} -\varepsilon\triangle u - (2 - x)u_x + \frac{3}{2}u &= f \quad \text{in } \Omega = (0,1)^2, \\ u &= 0 \quad \text{on } \partial\Omega, \end{aligned}$$

where the right-hand side f is chosen such that

$$u(x,y) = \left(\cos\frac{\pi x}{2} - \frac{\mathrm{e}^{-x/\varepsilon} - \mathrm{e}^{-1/\varepsilon}}{1-\mathrm{e}^{-1/\varepsilon}}\right)\frac{\left(1-\mathrm{e}^{-y/\sqrt{\varepsilon}}\right)\left(1-\mathrm{e}^{-(1-y)/\sqrt{\varepsilon}}\right)}{1-\mathrm{e}^{-1/\sqrt{\varepsilon}}}$$

is the solution. This problem was taken from [13] and considered also in [14]. The function u shows an exponential boundary layer near $x = 0$ and two characteristic boundary layers near $y = 0$ and $y = 1$, respectively.

All calculations were performed with the finite element package MooNMD [15]. The systems of linear equations which arise from the discretised problems were solved directly by using package UMFPACK [7–10].

In the following, 'order' will always denote the exponent α in a convergence order of form $O(N^{-\alpha})$ while 'ln-order' corresponds to the exponent α in a convergence order given by $O((N^{-1}\ln N)^{\alpha})$.

Table 3 shows for finite element spaces based on different finite elements the number of degrees of freedom (d.o.f.) and the number of non-zero entries in the corresponding system matrix (nnz). Since we are dealing with two-dimensional problems, both the number of degrees of freedom and the number of non-zero matrix entries increase roughly by a factor of 4 if the mesh parameter N is doubled.

All calculation have been performed with $p = 5$, i.e., the elements contain $\mathcal{P}_5$. All error norms were calculated by using the Gaussian quadrature formula with 8×8 points. The constant σ for defining the mesh transition points λ_x and λ_y was set to $p + 1 = 6$. The interpolation operator $\hat{J}$ on the reference cell $\hat{\tau}$ is based on an equidistant distribution of the evaluation points on the edges of $\hat{\tau}$.

In Tables 4 to 6 we present the results for the standard Galerkin discretisation and the local projection stabilisation on Shishkin meshes and Bakhvalov–Shishkin meshes. We will use $\varepsilon = 10^{-12}$ and the three finite element spaces based on Q_5^+, Q_5^*, and $Q_5^\oplus$, respectively. The stabilisation parameters δ_{11} and δ_{21} for the LPS method were chosen to the upper bound given by (3.9) with $C = 0.001$, i.e., the setting

$$\delta_{11} = 0.001N^{-2}(\max|\psi'|)^{10}, \qquad \delta_{21} = 0.001\varepsilon^{-1/2}\ln^{-1}N(N^{-1}\max|\psi'|)^2$$

was used since $p = 5$. We have chosen this constant C since larger values lead to worse results. This might be due to the fact that the stabilisation term s then dominates the discretisation.

Table 3: Number of degrees of freedom (d.o.f.) and number of non-zero matrix entries (nnz) for finite element spaces based on different finite elements.

	Q_5^+		Q_5^*		$Q_5^\oplus$	
N	d.o.f.	nnz	d.o.f.	nnz	d.o.f.	nnz
8	1,361	52,021	1,233	44,717	849	25,877
16	5,281	217,861	4,769	187,901	3,233	110,309
32	20,801	891,301	18,753	769,949	12,609	455,045
64	82,561	3,605,221	74,369	3,116,765	49,793	1,848,005
128	328,961	14,501,221	296,193	12,541,277	197,889	7,447,877

Table 4: Galerkin and LPS discretisation with Q_5^+ and $\varepsilon = 10^{-12}$.

	$\|\|\|u - \tilde{u}^N\|\|\|_\varepsilon$		Galerkin method		$\|\|\|J^N u - \tilde{u}^N\|\|\|_\varepsilon$				
	S-mesh			B–S mesh		S-mesh			B–S mesh	
N	error	order	ln-order	error	order	error	order	ln-order	error	order
8	1.262-03			7.017-05		9.355-04			5.186-05	
16	2.127-04	2.57	3.79	3.022-06	4.54	1.534-04	2.61	3.85	2.174-06	4.58
32	2.348-05	3.18	4.31	1.100-07	4.78	1.675-05	3.20	4.34	7.836-08	4.79
64	1.953-06	3.59	4.61	3.708-09	4.89	1.388-06	3.59	4.62	2.633-09	4.90
128	1.355-07	3.85	4.77	1.206-10	4.94	9.613-08	3.85	4.77	8.566-11	4.94

	$\|\|\|u - \tilde{u}^N\|\|\|_{LPS}$		LPS method		$\|\|\|J^N u - \tilde{u}^N\|\|\|_{LPS}$				
	S-mesh			B–S mesh		S-mesh			B–S mesh	
N	error	order	ln-order	error	order	error	order	ln-order	error	order
8	1.818-03			1.559-04		1.611-03			1.483-04	
16	3.275-04	2.47	3.65	4.725-06	5.04	2.924-04	2.46	3.63	4.207-06	5.14
32	3.490-05	3.23	4.38	1.419-07	5.06	3.060-05	3.26	4.42	1.187-07	5.15
64	2.356-06	3.89	5.00	4.512-09	4.97	1.895-06	4.01	5.16	3.677-09	5.01
128	1.538-07	3.94	4.88	1.415-10	5.00	1.194-07	3.99	4.94	1.132-10	5.02

As predicted by Theorem 6 the errors $\|\|\|u - \tilde{u}^N\|\|\|_\varepsilon$ for the Galerkin method and $\|\|\|u - u^N\|\|\|_\varepsilon$ for the LPS method converge with order 5 for all three elements. Although Theorem 6 gives error estimates for $\|\|\|u - u^N\|\|\|_\varepsilon$, we show the results in the stronger norm $\|\|\|u - u^N\|\|\|_{LPS}$. Comparing the results of the three different elements, we see that their differences are quite small. This means that even with less degrees of freedom and less non-zero matrix entries the same accuracy is obtained. Furthermore, it becomes obvious that the error norms on Bakhvalov–Shishkin meshes are much smaller than the corresponding norms on Shishkin meshes. This is caused by the logarithmic factor which is present only for Shishkin meshes.

For the closeness errors $\|\|\|J^N u - \tilde{u}^N\|\|\|_\varepsilon$ and $\|\|\|J^N u - u^N\|\|\|_\varepsilon$ the order 5 follows by combining the interpolation error and the results of Theorem 6. Contrary to the case of bilinear ansatz functions, see [14], the higher order case has no supercloseness property for the interpolation operator J^N.

In order to check the robustness of the error estimates, we varied $\varepsilon \in \{10^{-6}, 10^{-8}, 10^{-10}, 10^{-12}\}$ and fixed $N = 128$. Table 7 shows the errors $\|\|\|u - \tilde{u}^N\|\|\|_\varepsilon$ and $\|\|\|u - u^N\|\|\|_{LPS}$. It is obvious that the error is robust with respect to $\varepsilon \to 0$. Furthermore, the large difference between the results on Shishkin meshes and Bakhvalov–Shishkin meshes can be seen once more. On the same mesh, the differences between the results for the difference finite element spaces are again small.

Comparing the results obtained by the standard Galerkin discretisation and the local projection stabilisation, one finds that the difference in the numbers is quite small. Nevertheless, the error estimates for the local projection stabilisation are stronger since they provide additional control on the fluctuation of the derivative in streamline direction in the subdomains Ω_{11} and Ω_{21}.

Table 5: Galerkin and LPS discretisation with Q_5^* and $\varepsilon = 10^{-12}$.

$\left|\!\left|\!\left|u - \tilde{u}^N\right|\!\right|\!\right|_\varepsilon$ Galerkin method $\left|\!\left|\!\left|J^N u - \tilde{u}^N\right|\!\right|\!\right|_\varepsilon$

	S-mesh			B–S mesh		S-mesh			B–S mesh	
N	error	order	ln-order	error	order	error	order	ln-order	error	order
8	1.262-03			7.018-05		1.282-03	1.696		7.238-05	
16	2.127-04	2.57	3.79	3.022-06	4.54	2.194-04	2.547	3.76	3.153-06	4.52
32	2.348-05	3.18	4.31	1.100-07	4.78	2.453-05	3.161	4.29	1.156-07	4.77
64	1.953-06	3.59	4.61	3.708-09	4.89	2.054-06	3.578	4.60	3.908-09	4.89
128	1.355-07	3.85	4.77	1.204-10	4.94	1.429-07	3.846	4.76	1.271-10	4.94

$\left|\!\left|\!\left|u - \tilde{u}^N\right|\!\right|\!\right|_{LPS}$ LPS method $\left|\!\left|\!\left|J^N u - \tilde{u}^N\right|\!\right|\!\right|_{LPS}$

	S-mesh			B–S mesh		S-mesh			B–S mesh	
N	error	order	ln-order	error	order	error	order	ln-order	error	order
8	1.818-03			1.559-04		1.903-03	1.66		1.605-04	
16	3.275-04	2.47	3.65	4.725-06	5.04	3.498-04	2.44	3.60	4.864-06	5.04
32	3.490-05	3.23	4.38	1.419-07	5.06	3.754-05	3.22	4.37	1.469-07	5.05
64	2.356-06	3.89	5.00	4.512-09	4.98	2.562-06	3.87	4.98	4.685-09	4.97
128	1.433-07	4.04	5.00	1.412-10	5.00	1.548-07	4.05	5.01	1.472-10	4.99

Table 6: Galerkin and LPS discretisation with $Q_5^\oplus$ and $\varepsilon = 10^{-12}$.

$\left|\!\left|\!\left|u - \tilde{u}^N\right|\!\right|\!\right|_\varepsilon$ Galerkin method $\left|\!\left|\!\left|J^N u - \tilde{u}^N\right|\!\right|\!\right|_\varepsilon$

	S-mesh			B–S mesh		S-mesh			B–S mesh	
N	error	order	ln-order	error	order	error	order	ln-order	error	order
8	1.267-03			7.106-05		9.540-04			5.362-05	
16	2.144-04	2.56	3.78	3.058-06	4.54	1.578-04	2.60	3.83	2.264-06	4.57
32	2.381-05	3.17	4.30	1.113-07	4.78	1.745-05	3.18	4.31	8.195-08	4.78
64	1.991-06	3.58	4.60	3.749-09	4.89	1.465-06	3.57	4.60	2.760-09	4.89
128	1.389-07	3.85	4.76	1.217-10	4.94	1.023-07	3.84	4.76	8.967-11	4.94

$\left|\!\left|\!\left|u - \tilde{u}^N\right|\!\right|\!\right|_{LPS}$ LPS method $\left|\!\left|\!\left|J^N u - \tilde{u}^N\right|\!\right|\!\right|_{LPS}$

	S-mesh			B–S mesh		S-mesh			B–S mesh	
N	error	order	ln-order	error	order	error	order	ln-order	error	order
8	1.819-03			1.562-04		1.608-03			1.481-04	
16	3.279-04	2.47	3.65	4.752-06	5.04	2.926-04	2.46	3.63	4.232-06	5.13
32	3.502-05	3.23	4.38	1.430-07	5.05	3.077-05	3.25	4.41	1.209-07	5.13
64	2.383-06	3.88	4.99	4.546-09	4.97	1.941-06	3.99	5.13	3.767-09	5.00
128	1.461-07	4.03	4.99	1.423-10	5.00	1.119-07	4.12	5.10	1.161-10	5.02

Table 7: Robustness of Galerkin and LPS discretisation with $N = 128$.

Galerkin method

	Q_5^+		Q_5^*		$Q_5^\oplus$	
ε	S-mesh	BS-mesh	S-mesh	BS-mesh	S-mesh	BS-mesh
10^{-6}	1.887-07	1.714-10	1.905-07	1.713-10	9.138-07	5.859-10
10^{-8}	1.416-07	1.265-10	1.419-07	1.264-10	3.162-07	2.176-10
10^{-10}	1.360-07	1.211-10	1.361-07	1.209-10	1.628-07	1.333-10
10^{-12}	1.355-07	1.206-10	1.355-07	1.204-10	1.384-07	1.217-10

LPS method

	Q_5^+		Q_5^*		$Q_5^\oplus$	
ε	S-mesh	BS-mesh	S-mesh	BS-mesh	S-mesh	BS-mesh
10^{-6}	1.943-07	1.719-10	1.914-07	1.718-10	9.143-07	5.859-10
10^{-8}	1.583-07	1.305-10	1.451-07	1.296-10	3.182-07	2.192-10
10^{-10}	1.646-07	1.348-10	1.411-07	1.331-10	1.666-07	1.452-10
10^{-12}	1.538-07	1.415-10	1.433-07	1.412-10	1.461-07	1.423-10

6. Conclusions

We have shown for a general class of finite element spaces based on local function spaces $\widehat{\mathcal{E}}(\hat{\tau})$ with $\mathcal{P}_p(\hat{\tau}) \subset \widehat{\mathcal{E}}(\hat{\tau}) \subset \mathcal{Q}_p(\hat{\tau})$ that local anisotropic error estimates exist for a vertex-edge-cell and point-value oriented interpolation operators. This enabled us to apply already known convergence results on S-type meshes to prove ε-uniformly convergence of order p of the Galerkin FEM and the LPSFEM in the ε-weighted energy norm, and a robust supercloseness property of the LPSFEM in the stronger LPS-norm.

The numerical results showed that the numerical errors of the different spaces on the same mesh are comparable. However, the errors on Shishkin meshes are much larger than the corresponding errors on Bakhvalov–Shishkin meshes. On the finest meshes in our calculations, the difference was about three orders of magnitude.

We were using rectangular meshes. It is known for general quadrilateral meshes that the convergence order of serendipity elements can decrease, see [4] for an approximation theory of quadrilateral finite elements. Following this analysis our results should hold true for meshes of parallelograms too.

The presented consideration for a singularly perturbed problem with one exponential and two characteristic boundary layers can be extended with a few modifications to problems with exponential boundary layers only. This will be subject of a forthcoming study.

Acknowledgements

We would like to thank the referees for their valuable comments and constructive criticism that helped to improve the paper.

References

[1] G. Acosta, T. Apel, R. G. Durán, and A. L. Lombardi. Anisotropic error estimates for an interpolant defined via moments. *Computing*, 82:1–9, 2008.

[2] T. Apel. *Anisotropic finite elements: local estimates and applications*. Advances in Numerical Mathematics. B. G. Teubner, Stuttgart, 1999.

[3] D. N. Arnold and G. Awanou. The serendipity family of finite elements. submitted to Found. Comput. Math., 2010.

[4] D. N. Arnold, D. Boffi, R. S. Falk, and L. Gastaldi. Finite element approximation on quadrilateral meshes. *Comm. Numer. Methods Engrg.*, 17(11):805–812, 2001.

[5] N. S. Bakhvalov. The optimization of methods of solving boundary value problems with a boundary layer. *U.S.S.R. Comput. Math. Math. Phys.*, 9(4):139–166, 1969.

[6] R. Becker and M. Braack. A finite element pressure gradient stabilization for the Stokes equations based on local projections. *Calcolo*, 38(4):173–199, 2001.

[7] T. A. Davis. Algorithm 832: UMFPACK V4.3—an unsymmetric-pattern multifrontal method. *ACM Trans. Math. Software*, 30(2):196–199, 2004.

[8] T. A. Davis. A column pre-ordering strategy for the unsymmetric-pattern multifrontal method. *ACM Trans. Math. Software*, 30(2):167–195, 2004.

[9] T. A. Davis and I. S. Duff. An unsymmetric-pattern multifrontal method for sparse *LU* factorization. *SIAM J. Matrix Anal. Appl.*, 18(1):140–158, 1997.

[10] T. A. Davis and I. S. Duff. A combined unifrontal/multifrontal method for unsymmetric sparse matrices. *ACM Trans. Math. Software*, 25(1):1–20, 1999.

[11] S. Franz. Continuous interior penalty method on a shishkin mesh for convection-diffusion problems with characteristic boundary layers. *Comput. Meth. Appl. Mech. Engng.*, 197(45-48):3679–3686, 2008.

[12] S. Franz. *Singularly perturbed problems with characteristic layers: Supercloseness and postprocessing*. PhD thesis, Department of Mathematics, TU Dresden, 2008.

[13] S. Franz, T. Linß, and H.-G. Roos. Superconvergence analysis of the SDFEM for elliptic problems with characteristic layers. *Appl. Numer. Math.*, 58(12):1818–1829, 2008.

[14] S. Franz and G. Matthies. Local projection stabilisation on S-type meshes for convection-diffusion problems with characteristic layers. *Computing*, 87(3–4):135–167, 2010.

[15] V. John and G. Matthies. MooNMD - a program package based on mapped finite element methods. *Comput. Vis. Sci.*, 6(2–3):163–170, 2004.

[16] T. Linß. An upwind difference scheme on a novel Shishkin-type mesh for a linear convection-diffusion problem. *J. Comput. Appl. Math.*, 110(1):93–104, 1999.

[17] T. Linß. Analysis of a Galerkin finite element method on a Bakhvalov-Shishkin mesh for a linear convection-diffusion problem. *IMA J. Numer. Anal.*, 20(4):621–632, 2000.

[18] T. Linß and M. Stynes. Numerical methods on Shishkin meshes for linear convection-diffusion problems. *Comput. Methods Appl. Mech. Eng.*, 190(28):3527–3542, 2001.

[19] G. Matthies. Local projection methods on layer-adapted meshes for higher order discretisations of convection-diffusion problems. *Appl. Numer. Math.*, 59(10):2515–2533, 2009.

[20] G. Matthies. Local projection stabilisation for higher order discretisations of convection-diffusion problems on Shishkin meshes. *Adv. Comput. Math.*, 30(4):315–337, 2009.

[21] G. Matthies, P. Skrzypacz, and L. Tobiska. A unified convergence analysis for local projection stabilisations applied to the Oseen problem. *M2AN Math. Model. Numer. Anal.*, 41(4):713–742, 2007.

[22] J. Melenk. *hp-Finite Element Methods for Singular Perturbations*, volume 1796 of *Lecture Notes in Mathematics*. Springer, Berlin, 2003.

[23] J. J. H. Miller, E. O'Riordan, and G. I. Shishkin. *Fitted numerical methods for singular perturbation problems: Error estimates in the maximum norm for linear problems in one and two dimensions*. World Scientific Publishing Co. Inc., River Edge, NJ, 1996.

[24] H.-G. Roos and T. Linß. Sufficient conditions for uniform convergence on layer-adapted grids. *Computing*, 63(1):27–45, 1999.

[25] M. Stynes and E. O'Riordan. A uniformly convergent Galerkin method on a Shishkin mesh for a convection-diffusion problem. *J. Math. Anal. Appl.*, 214(1):36–54, 1997.
[26] M. Stynes and L. Tobiska. Using rectangular Q_p elements in the SDFEM for a convection-diffusion problem with a boundary layer. *Appl. Numer. Math.*, 58(12):1709–1802, 2008.
[27] B. Szabó and I. Babuška. *Finite Element Analysis*. John Wiley and Sons, New York, 1991.